

## Traversing the “Top-Down/Bottom-Up” Divide: Molecular-Scale Lithography of Self-Assembled Ribbons

Jonas Jarvholm,<sup>†</sup> Mohan Srinivasarao,<sup>†,‡</sup> and Laren M. Tolbert<sup>\*,†</sup>

School of Chemistry and Biochemistry and School of Polymer, Textile, and Fiber Engineering, Georgia Institute of Technology, Atlanta, Georgia 30332-0400

Received July 9, 2008; E-mail: laren.tolbert@chemistry.gatech.edu

Moore’s Law has successfully described the trend in increasing transistor density for integrated circuits in the semiconductor industry for over five decades.<sup>1</sup> Improvements in photolithography now allow production of silicon structures as small as 45 nm with acceptable defect levels. Further improvements require the use of shorter wavelength tools (EUV), immersion methods, and complicated optical methods, including two-wavelength lithography and optical interference, all of which are subject, within limits, to the Rayleigh equation.<sup>2</sup>

$$hp = (k_1\lambda)/n \sin \theta \quad (1)$$

Whether such “top-down” methods will allow the Moore’s Law plot to continue is still the subject of some controversy.<sup>3</sup> More recently, “bottom-up” methods are emerging, including the use of block copolymers to produce regular patterns in which the different components have differential dissolution rates, allowing selective etching into the underlying Si structures.<sup>4</sup> We now report technology for which the feature size of patterns is dependent on the molecular size rather than either the numerical aperture or the periodicity of a polymer

The “bottom-up” approach, requiring a molecular methodology, itself presents formidable synthetic and systems engineering challenges. Since the Rayleigh limit is primarily one of exposure tools used for photolithography, we propose instead a concept for which the feature size is not limited by wavelength. The pattern is created not by a photoresist but rather by a monolayer of highly stable self-organizing molecules. By using this organized monolayer directly as an etch-mask (a “molecular mask”) the photolithographic process is essentially bypassed while maintaining the advantages of the Si manufacturing infrastructure (Figure 1). This allows the ultimate resolution for all types of lithography to be approached, that is, the outlines of individual molecules in Si/SiO<sub>2</sub>. A similar approach involved the use of DNA molecules as the organizing principle, in which the DNA pattern is transferred to Au,<sup>5</sup> or carbon nanotubes are used as a patterning material.<sup>6</sup> In our case, we use an aromatic liquid crystalline material (**C96**) directly to successfully transfer a monolayer of 4 nm wide molecular structures into the substrate. The monolayer is covalently bound to the surface to allow monolayer fabrication and increase the stability of the system toward an etching (fluorine) plasma. Significantly the feature size does not depend on the Rayleigh limit but only on the size of the self-assembled structures. This is also the first report to our knowledge for which a molecular monolayer is robust enough to act directly as an etch resist.

**C96** belongs to a class of large graphitic molecules which are both polycyclic aromatic hydrocarbons (PAHs) and discotic liquid crystals.<sup>7,8</sup> The liquid crystalline behavior is facilitated by the presence of dodecyl

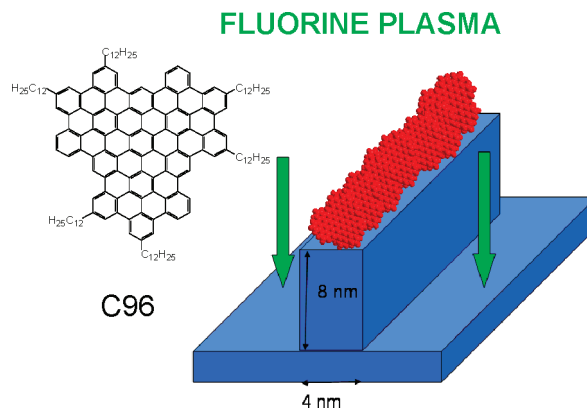


Figure 1. Structure of **C96** and schematic of molecular lithography.

chains along the periphery of the disk which allow solubility in organic solvents. **C96** and other graphitic materials have been studied extensively since their preparation by differential scanning calorimetry, X-ray diffraction, and solid-state NMR to determine the properties, dynamics, and arrangements of these discotic materials.<sup>9–14</sup> Such PAHs have many useful properties, including high charge carrier mobility and long-range self-organization.<sup>15</sup> **C96** self-assembles into 1-D columnar supramolecular structures due to the  $\pi$ – $\pi$  interaction between the core aromatic regions.<sup>16,17</sup> PAHs are known to organize into highly ordered layers using Langmuir–Blodgett deposition,<sup>18</sup> zone casting,<sup>19</sup> zone crystallization,<sup>20</sup> or solution casting onto prealigned polytetrafluoroethylene.<sup>21</sup> Pisula et al.<sup>6</sup> suggest the distance between the cores of **C96** is 0.34–0.36 nm which resembles the distance of interlayer graphite (0.34 nm). From these data it has been predicted that the columns have nearly the same density as graphite,  $\rho_c = 2.25$  g/cm.<sup>6</sup>

Molecular lithography depends on the stability of the monolayer toward a fluorine plasma to transfer the molecular patterns into the substrate. The stability of a resist or molecule in a dry etch process has been studied and is described by the Ohnishi<sup>22</sup> and Ring<sup>23</sup> parameters, which is related to the carbon content of the resist. Although thin-layer resists based upon highly aromatic materials are known, both parameters suggest that **C96** is an ideal candidate as a molecular resist.

On clean thermally grown SiO<sub>2</sub>, ~500 nm thick, a monolayer of **C96** fibers was created by photochemical attachment to an immobilized self-assembled monolayer (SAM) of a silane benzophenone derivative.<sup>24–27</sup> The free **C96** was removed with toluene via Soxhlet extraction with toluene, leaving a **C96** submonolayer of **C96** fibers. Using SEM and AFM, the width of the fibers was measured to be ~4 nm: approximately the width of 1–2 molecules. AFM analysis showed that the height of the **C96** fibers,  $2.1 \pm 0.2$  nm, corresponded to the calculated diameter of the molecule. The sample was placed in a Vision 320-RIE and subjected to a soft etch, created at a plasma microwave

<sup>†</sup> School of Chemistry and Biochemistry.

<sup>‡</sup> School of Polymer, Textile, and Fiber Engineering.

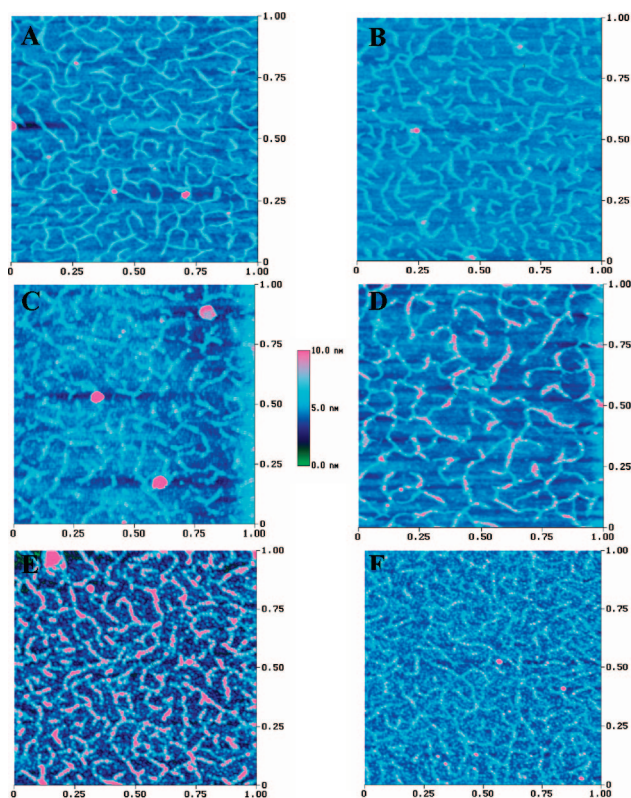


**Figure 2.** AFM results from etch experiments. (A) **C96** fibers pre-etch, CA = 83°. (b) After 15 s etch, CA = 80°. (c) After 15 s etch and piranha treatment, CA = 9°. (d–f) After both etch and piranha treatment, CA = 9°. (d) – 30 s of etching. (e) – 45 s of etching. (f) 60 s etch. Height scales are 10 nm except for B which is 20 nm. Width scales are 10 nm.

power of 75 W using CF<sub>4</sub> at 31 sccm, H<sub>2</sub> at 3 sccm, and 50 mTorr. The etch rate in SiO<sub>2</sub> was  $91 \pm 3 \text{ \AA}/\text{min}$  via ellipsometry. A soft plasma was chosen to maximize the lifetime of the **C96** fibers while still etching SiO<sub>2</sub>. The **C96** fiber “mask” was removed with a piranha solution (70% H<sub>2</sub>SO<sub>4</sub>, 30% H<sub>2</sub>O<sub>2</sub>), for 1 h, and rinsed with deionized H<sub>2</sub>O. AFM analysis before and after etching revealed the persistent shape of the features but with various heights, depending on the etch time. The height of the structures after etching was the sum of those of the SiO<sub>2</sub> structures and **C96** and decreased upon piranha treatment by the height of the **C96** molecules. A series of different etch times followed by piranha treatment were performed: 15, 30, 45, and 60 s. The height  $h$  increased with increased etch times. After 15 s,  $h = 4.7 \pm 0.3 \text{ nm}$ ; after piranha treatment,  $h = 2.5 \pm 0.2 \text{ nm}$ , corresponding to the diameter and initial size of the **C96** fibers. For a 30 s etch,  $h = 6.2 \pm 0.4 \text{ nm}$ , decreasing to  $4.8 \pm 0.3 \text{ nm}$ . For 45 s,  $h = 8.5 \pm 0.5 \text{ nm}$ , decreasing to  $8.1 \pm 0.5 \text{ nm}$ . After a 60 s etch,  $h$  started to decrease compared to the 45 s etch, and  $h$ , at  $4.2 \pm 0.5 \text{ nm}$ , did not change upon piranha treatment (Figure 2), indicating degradation of **C96**. In addition, the **C96** SAM static water contact angle of  $83 \pm 2^\circ$  decreased to  $63 \pm 4^\circ$  after 45 s of etch. All samples had a contact angle of  $9 \pm 2^\circ$  upon piranha treatment suggesting a pure SiO<sub>2</sub> surface. The C content observed by XPS decreased with increasing etch times, while the Si content increased (see Figure S2 for both contact angle and XPS results). The aspect ratio (height/width) of the tallest features was  $\sim 2$ . The etch ratio of SiO<sub>2</sub>/**C96** was 4:1, compared to photoresists that normally have etch ratios of  $\sim 1:1$ .<sup>28</sup> After piranha treatment the C content was similar to the adventitious C detected on a blank SiO<sub>2</sub> surface.

**C96** is an ideal candidate for molecular lithography, providing fused aromatic rings with excellent etch resistance toward fluorine

plasma. Both the  $O$  and  $R$  parameters suggest good resist stability,  $O = 1.89$  and  $R = 0.53$  (traditional photoresists have an  $O$  parameter of 2.5–5).<sup>22</sup> The  $\pi$ -stacking discotic liquid crystal **C96** serves as the first example of a “molecular” etch resist, organized in this case by liquid crystalline order and establishing the principle of extensive graphitic molecules as etch barriers. Thus the size of the features created is no longer dependent on the diffraction limit but rather on the size and organization of individual molecules. Note that resolution in conventional photoresists is defined either by distance between features or by feature size, and we are referring only to the latter. Of course, implementation of this technology in functional devices will require usable patterns, for instance, using technologies such as dip-pen lithography<sup>29</sup> or DNA-like self-organization. However, this changes the task from photolithography to organic synthesis.

**Acknowledgment.** We thank Prof. Klaus Müllen for **C96** and both him and Prof. Clifford Henderson for helpful discussions. This work was supported by grants from the U.S. NSF (CMMI-0600600) and Semiconductor Research Corporation.

**Supporting Information Available:** Experimental Section. This material is available free of charge via the Internet at <http://pubs.acs.org>.

## References

- (1) Steelher, J. *J. Chem. Educ.* **2007**, *84*, 1278.
- (2) Gil, D.; Brunner, T.; Fonseca, C.; Seong, N.; Streefkerk, B.; Wagner, C.; Stavenga, M. *J. Vac. Sci. Technol., B* **2004**, *34*(3), 3431. hp = half pitch,  $k_1$  = resolution constant,  $\lambda$  = wavelength,  $n$  = refractive index,  $\sin \theta$  = angle of light relative to the surface.
- (3) Resnick, D. J.; Mancini, D.; Dauksher, W. J.; Nordquist, K.; Bailey, T. C.; Johnson, S.; Sreenivasan, S. V.; Wilson, C. G. *Microelectron. Eng.* **2003**, *69*, 412.
- (4) Ruiz, R.; Kang, H.; Detcheverry, F. A.; Dobisz, E.; Kercher, D. S.; Albrecht, T. R.; de Pablo, J. J.; Nealey, P. F. *Science* **2008**, *321*, 936–939.
- (5) Deng, Z.; Mao, C. *Angew. Chem., Int. Ed.* **2004**, *43*, 4068–4070.
- (6) Chae, J.; Ho, X.; Rogers, J. A.; Jain, K. *Proc. SPIE* **2008**, *7037* (Carbon Nanotubes and Associated Devices), 70370M/1–70370M/8.
- (7) Tomovic, Z.; Watson, M. D.; Müllen, K. *Angew. Chem., Int. Ed.* **2004**, *43*, 755.
- (8) Pisula, W.; Tomovic, Z.; Simpson, C.; Kastler, M.; Pakula, T.; Müllen, K. *Chem. Mater.* **2005**, *17*, 4296.
- (9) Fischbach, I.; Pakula, T.; Minkin, P.; Fechtenkötter, A.; Müllen, K.; Speiss, H. W.; Saalwachter, K. *J. Phys. Chem. B* **2002**, *106*, 6408.
- (10) Tchebotareva, N.; Yin, X. M.; Watson, M. D.; Samori, P.; Rabe, J.; Müllen, K. *J. Am. Chem. Soc.* **2003**, *125*, 9734.
- (11) Fischbach, I.; Ebert, F.; Speiss, H. W.; Schnell, I. *Chemphyschem* **2004**, *5*, 895.
- (12) Wu, J. S.; Watson, M. D.; Zhang, L.; Wang, Z. H.; Müllen, K. *J. Am. Chem. Soc.* **2004**, *126*, 177.
- (13) Fechtenkötter, A.; Saalwachter, K. J.; Habison, M. A.; Müllen, K.; Speiss, H. W. *Angew. Chem., Int. Ed.* **1999**, *38*, 3039.
- (14) Herwig, P.; Kayser, C. W.; Müllen, K.; Speiss, H. W. *Adv. Mater.* **1996**, *8*, 510.
- (15) Van de Craats, A. M.; Warman, J. M. *Adv. Mater.* **2001**, *13*, 130.
- (16) Engelkamp, H.; Middelbeek, S.; Nolte, R. *Science* **1999**, *284*, 785.
- (17) Bushby, R.; Boden, N.; Kilner, C.; Lozman, O.; Lu, Z.; Liu, Q.; Thornton-Pett, M. *J. Mater. Chem.* **2003**, *13*, 470.
- (18) Reizel, N.; Hassenkam, T.; Balashev, K.; Jensen, T. R.; Howes, P. B.; Fechtenkötter, A.; Tchebotareva, N.; Ito, S.; Müllen, K.; Bjornholm, T. *Chem.–Eur. J.* **2001**, *7*, 4894.
- (19) Tracz, A.; Jeszka, J. K.; Watson, M. D.; Pisula, W.; Müllen, K.; Pakula, T. *J. Am. Chem. Soc.* **2003**, *125*, 1682.
- (20) Liu, C. Y.; Bard, A. J. *Chem. Mater.* **2000**, *12*, 2353.
- (21) Bunk, O.; Nielsen, M. M.; Solling, T. I.; van de Craats, A. M.; Stutzmann, J. *J. Am. Chem. Soc.* **2003**, *125*, 2252.
- (22) Gokan, H.; Esho, S.; Ohnishi, Y. *J. Electrochem. Soc.* **1983**, *130* (1), 143.
- (23) Kunz, R.; Palmateer, S.; Forte, A.; Allen, R.; Wallraff, G.; DiPietro, A.; Hofer, D. *Proc. SPIE–Int. Soc. Opt. Eng.* **1996**, *2724*, 365.
- (24) Claisses, L.; Eisleb, O. *Liebigs Ann. Chem.* **1913**, *401*, 21.
- (25) Speier, J. L. *Adv. Organomet. Chem.* **1979**, *17*, 407.
- (26) Prucker, O.; Naumann, C. A.; Rühle, J.; Knoll, W.; Frank, C. W. *J. Am. Chem. Soc.* **1999**, *121*, 8766.
- (27) Turro, N. *Modern Molecular Photochemistry*; University Science Books: Mill Valley, CA, 1991.
- (28) Lee, C.; Park, C.; Lee, N. *Microelectron. Eng.* **2007**, *84*, 165.
- (29) AFM nanolithography is itself proving to provide useful structures on the molecular length scale: Martinez, J.; Martinez, R. V.; Garcia, R. *Nano Lett.* **2008**, *8*, 3636–3639.

JA805319K